Effect of magnetostatic interactions on the hysteresis parameters of single-domain and pseudo-single-domain grains

Effect of magnetostatic interactions on the hysteresis parameters of single-domain and pseudo-single-domain grains

Adrian Muxworthy, Wyn Williams, and Davinder Virdee
Institute of Earth Sciences, University of Edinburgh, Edinburgh, UK

Received 15 May 2003; revised 5 August 2003; accepted 18 August 2003; published 7 November 2003.

[1] From experiments it is known that magnetostatic interactions between grains strongly affect the magnetic behavior of samples. However, because of the difficulty in predicting the nonlinear behavior, the effect of interactions has been largely ignored from theoretical models. Instead models are often based on noninteracting assemblages. This approximation is valid for certain natural systems, but there are many cases where interactions are known to be important, for example, bacterial magnetosomes found in sedimentary rocks. Using a three-dimensional micromagnetic model, we have conducted a detailed study of the role of magnetostatic interactions on the magnetic properties of assemblages of ideal single domain (SD) grains and cubic grains between 30–250 nm in size. We quantify the contribution of interactions to hysteresis parameters and the Day plot. We show that interactions can strongly affect the magnetic characteristics of a grain assemblage. For example, assemblages of interacting SD grains can plot in the traditional multidomain (MD) area of the Day plot. For grains >100 nm in size, interactions can have the opposite effect, and can cause the hysteresis parameters to shift toward the SD region of the Day plot. In addition to varying grain size, we have also considered various anisotropies, e.g., uniaxial and cubic, and the importance of the alignment configuration of the particle assemblages, i.e., randomly distributed or aligned. It is shown that for assemblages of aligned magnetite particles, that as the interaction spacing is decreased, the SD/MD transition size increases, which may explain why some magnetotatic bacteria possess aligned grains of magnetite above the traditional transition size value of 70 nm. By aligning the anisotropies, the grains become stable SD, and having larger crystals will increase the magnetic signal. *INDEX TERMS:* 1512 Geomagnetism and Paleomagnetism: Environmental magnetism; 1518 Geomagnetism and Paleomagnetism: Magnetic fabrics and anisotropy; 1521 Geomagnetism and Paleomagnetism: Paleointensity; 1540 Geomagnetism and Paleomagnetism: Rock and mineral magnetism; 3230 Mathematical Geophysics: Numerical solutions; *KEYWORDS:* magnetostatic interactions, micromagnetism, magnetite, magnetic hysteresis

Citation: Muxworthy, A., W. Williams, and D. Virdee, Effect of magnetostatic interactions on the hysteresis parameters of single-domain and pseudo-single-domain grains, *J. Geophys. Res.*, *108*(B11), 2517, doi:10.1029/2003JB002588, 2003.

1. Introduction

[2] In rock magnetism the interpretation of a magnetic measurement is based on our understanding of the fundamental behavior of common magnetic minerals. Many aspects of natural magnetic minerals, e.g., variation in stoichiometry and grains size, and their standard magnetic properties, e.g., hysteresis, have been rigorously studied. Most of our interpretation of a rock magnetic signal is based on models of either single crystals or assemblages of magnetically noninteracting grains. Yet, in nature, it is rare that samples are truly noninteracting; for example, bacterial magnetosomes found in sedimentary rocks are known to be strongly interacting and can contribute significantly to the magnetic signature [*McCartney et al.*, 2001].

[3] Magnetostatic interactions are known to be important; there is much direct experimental evidence in the physics literature showing that interactions strongly affect the magnetic signal [e.g., *Hwang et al.*, 2000; *Ross et al.*, 2002]. However, the contribution of magnetostatic interactions has been largely ignored from rock magnetic interpretations or only qualitatively acknowledged. There have been only a limited number of experimental rock magnetic studies where the interaction spacing has been accurately controlled [*King et al.*, 1996; *King and Williams*, 2000].

[4] The main reason that interactions have been largely ignored from theoretical models, is because the behavior of nonuniform magnetic structures, i.e., large single domain (SD) grains, interacting SD grains and larger grains, i.e., pseudo-single-domain (PSD) and multidomain (MD) (Figure 1), is highly nonlinear making it difficult to determine. With the rapid advance in computing power, it has become increasingly possible to directly model such behav-

0148-0227/03/2003JB002588$09.00

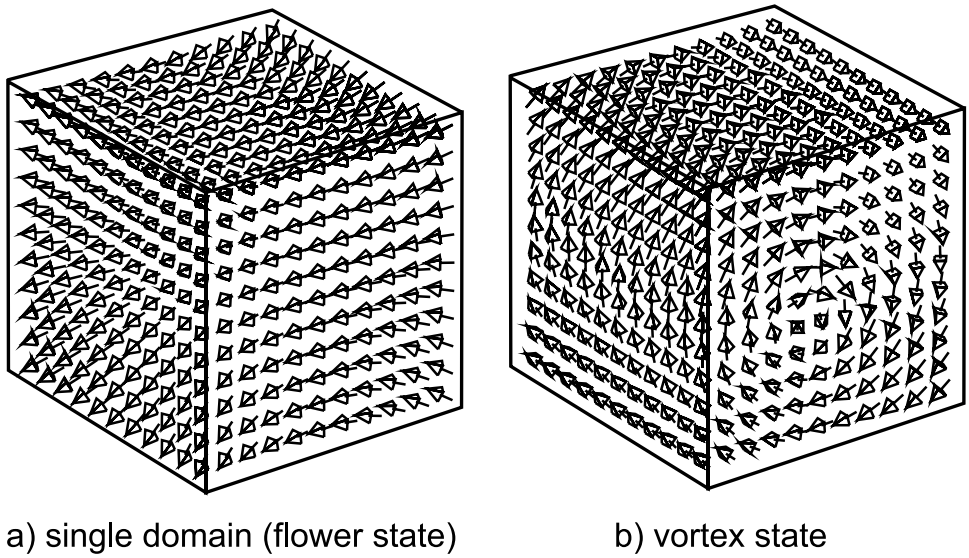

Figure 1. Domains states occurring in cubic grains of magnetite at room temperature for a grain with edge length of 100 nm (a) single domain (flower state) and (b) single vortex state. In this paper the term "SD state" refers not just to homogeneous magnetization structures as in Néel theory, but also to nonuniform domain structures as shown in (a) which are basically SD-like with a degree of flowering toward the edges of the grain. The [001] axis aligns with the z axis of the cube.

ior by implementing *Brown*'s [1963] micromagnetic formalism. Noninteracting uniform SD grains can be very well explained by analytical theories [*Stoner and Wohlfarth*, 1948; *Néel*, 1949].

[5] There have been several rock magnetic micromagnetic studies which have looked at many features of SD and PSD behavior, for example, hysteresis [*Williams and Dunlop*, 1995; *Muxworthy and Williams*, 1999] and thermoremanence acquisition [*Winklhofer et al.*, 1997; *Muxworthy et al.*, 2003]. All of these studies have been for isolated single crystals, i.e., effectively noninteracting grains. Previous theoretical rock magnetic studies examining interactions have considered only ideal SD grains, and have used either analytical or dipolar approximations [e.g., *Dunlop and West*, 1969; *Davis*, 1980; *Sprowl*, 1990; *Muxworthy*, 2001], or Monte Carlo simulations [*Shcherbakov et al.*, 1995, 1996, 2000].

[6] In this paper the effects of interactions on the hysteresis parameters of cubic grains of magnetite and magnetite-like minerals are examined using a three-dimensional (3D) micromagnetic model. We concentrate on the effect of interactions on various grain sizes and anisotropies. In two future papers, the effect on interactions on differing grain shapes and on assemblages of mixed mineralogy will be considered.

2. The Micromagnetic Model

[7] The basic algorithm used to calculate the results in this paper was fully described by *Wright et al.* [1997]. The model subdivides a grain into a number of finite element sub-cubes. Each sub-cube represents the averaged magnetization direction of many hundreds of atomic magnetic dipole moments. All the sub-cubes have equal magnetic magnitude, but their magnetization can vary in direction. The domain structure is calculated by minimizing the total magnetic energy E_{tot}, which is the sum of the exchange energy E_{ex}, the magnetostatic energy E_d and the anisotropy E_{anis} [*Brown*, 1963]. E_d is calculated using fast-Fourier transforms (FFT); this type of micromagnetic model allows the high resolution needed to examine arrays of interacting grains. The domain state of a grain is calculated by minimizing E_{tot} by the conjugate-gradient method to give the local energy minimum (LEM).

[8] In the model $E_{ex} \propto$ the exchange constant A, $E_d \propto$ the spontaneous magnetization M_S and $E_{anis} \propto$ the first magnetocrystalline anisotropy K_1. Values for A, M_S and K_1 were taken from *Heider and Williams* [1988], *Pauthenet and Bochirol* [1951] and *Fletcher and O'Reilly* [1974] respectively. Even though the model conditions are set for a magnetite-like material at room temperature, the exclusion of thermal agitation in the model means that we are effectively modeling at 0 K.

[9] The magnetostrictive anisotropy was not included in the model because there are as yet unresolved technical difficulties in incorporating it for spatially independent crystals [*Fabian and Heider*, 1996]. However, *Fabian and Heider* [1996] showed that for magnetite grains <5000 nm in size, this omission should be insignificant at room temperature. The structures in this study were calculated for stress-free samples, i.e., no dislocations and no external stress, making the contribution from the magnetoelastic anisotropy zero.

[10] In an assemblage of grains each particle experiences, in addition to any external field, fields generated by neighboring particles [*Dunlop and West*, 1969]. The field generated from a stable SD grain is relatively constant compared to the time it takes for a SD grain to rotate in the field. This makes it possible to treat such interactions as static [*Spinu and Stancu*, 1998]. Smaller superparamagnetic

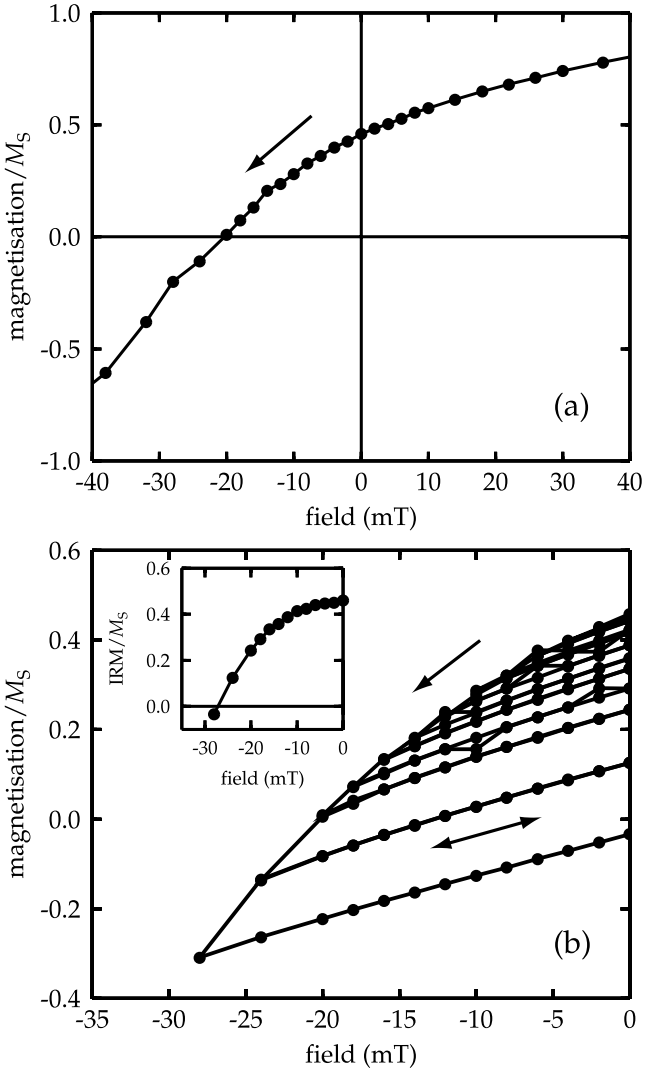

Figure 2. (a) A simulated hysteresis curve and (b) a H_{CR} determination, i.e., multiple increasing minor loops until the remanent magnetization is less than zero. Inset in (b) shows the remanent magnetization versus maximum field. The model is for a uniaxial random assemblage of ideal SD grains with d = 1. M_{RS}/M_S was found to be 0.43, H_C was 20.3 mT, and H_{CR} determined to be 27.2 mT.

(SP) grains are unstable due to the influence of thermal agitation, and the interaction field associated with such particles is not constant during the time it takes for a neighboring interacting magnetic moment to flip. Such dynamic interactions are relatively larger than static interaction fields [e.g., *Dormann et al.*, 1988]. Dynamic interactions are only important for grains near the blocking volume, which for magnetite at room temperature is ~30 nm [*Dunlop*, 1973]; though the blocking volume itself is dependent on interactions [e.g., *Dormann et al.*, 1988; *Muxworthy*, 2001].

[11] In this paper we consider only static interactions. First, because we do not include thermal agitation in our model, i.e., there is no SP/stable-SD transition size in our model, and Second because we are primarily interested in remanence carrying grains.

[12] Modeling interactions in this paper was simply done by masking-out blank cells [*Virdee*, 1999].

3. Interactions Between Uniform Single-Domain (SD) Particles

[13] By considering ideal SD particles with uniform internal magnetic structure, it is possible to model large numbers of grains. We have simulated hysteresis for assemblages of 1000 SD grains (10 × 10 × 10 grid) with randomly orientated magnetocrystalline anisotropy. We consider the effect of variations in interaction spacing d, and order and type of magnetocrystalline anisotropy. The different types of anisotropy can be roughly split into two groups; First, anisotropy which is evenly distributed in three dimensions ("nonplanar"), e.g., magnetite's cubic anisotropy, second anisotropy lying in the basal plane ("planar") due to a very high out of basal-plane anisotropy, e.g., hematite. Three different nonplanar magnetocrystalline anisotropies were modeled; uniaxial, cubic with $K_1 > 1$ (six fold symmetry), like metallic iron, and cubic with $K_1 < 1$ (eight fold symmetry), e.g., magnetite, and two planar anisotropies; uniaxial (b-uniaxial) and trigonal. K_1 was kept constant for all six anisotropies.

[14] A representative partial hysteresis curve and a remanent coercive force (H_{CR}) determination for the uniaxial regime with d = 1 are shown in Figure 2. From Figure 2a the coercive force (H_C) was determined to be 20.3 mT and the reduced saturation isothermal remanence (M_{RS}/M_S) was 0.46. H_{CR} was found to be 27.2 mT (Figure 2b). d is the distance between each cell as a function of the normalized grain size, e.g., d = 0.5 represents a spacing half the grain size.

[15] In Figure 3, the M_{RS}/M_S, H_C and H_{CR} are plotted versus d for assemblages with different anisotropy regimes. There are some consistent effects of interactions; as d increases M_{RS}/M_S increases from a minimum at d = 0 to a maximum at d = 5 (Figure 3a). For the nonplanar anisotropies $M_{RS}/M_S \sim 0$ at d = 0. At some point for $d_{M_{RS}}$ between d = 0 and 5, M_{RS}/M_S becomes independent on interaction spacing; $d_{M_{RS}}$ is dependent on the type of anisotropy. H_C for the nonplanar anisotropies displays a similar behavior to M_{RS}/M_S, increasing with d until saturation at d_{H_C} (Figure 3b). H_C does not equal zero at d = 0. The behavior of H_C with d for the planar anisotropies is noisier and does not display a strong dependency on d. H_{CR} displays no strong dependency on d, though there is a small gradual decrease in H_{CR} with increasing d (Figure 3c). The behavior of these hysteresis parameters with increasing interactions is similar to those predicted by simpler Stoner-Wohlfarth (SW) models [e.g., *Bertram and Bhatia*, 1973; *Davis*, 1980; *Sprowl*, 1990].

3.1. Testing the Model

[16] It is possible to compare M_{RS}/M_S for the completely noninteracting regimes, i.e., d = 5, with analytically determined values. For d = 5, we estimated M_{RS}/M_S = 0.50 for uniaxial anisotropy, which agrees with the theoretical estimates [*Wohlfarth and Tonge*, 1957; *Dunlop*, 1971; *Tauxe et al.*, 2002]. Similarly for cubic symmetry with $K_1 > 0$, M_{RS}/M_S was 0.83 and for $K_1 < 0$ we found M_{RS}/M_S = 0.86, compared to analytical estimates of 0.831

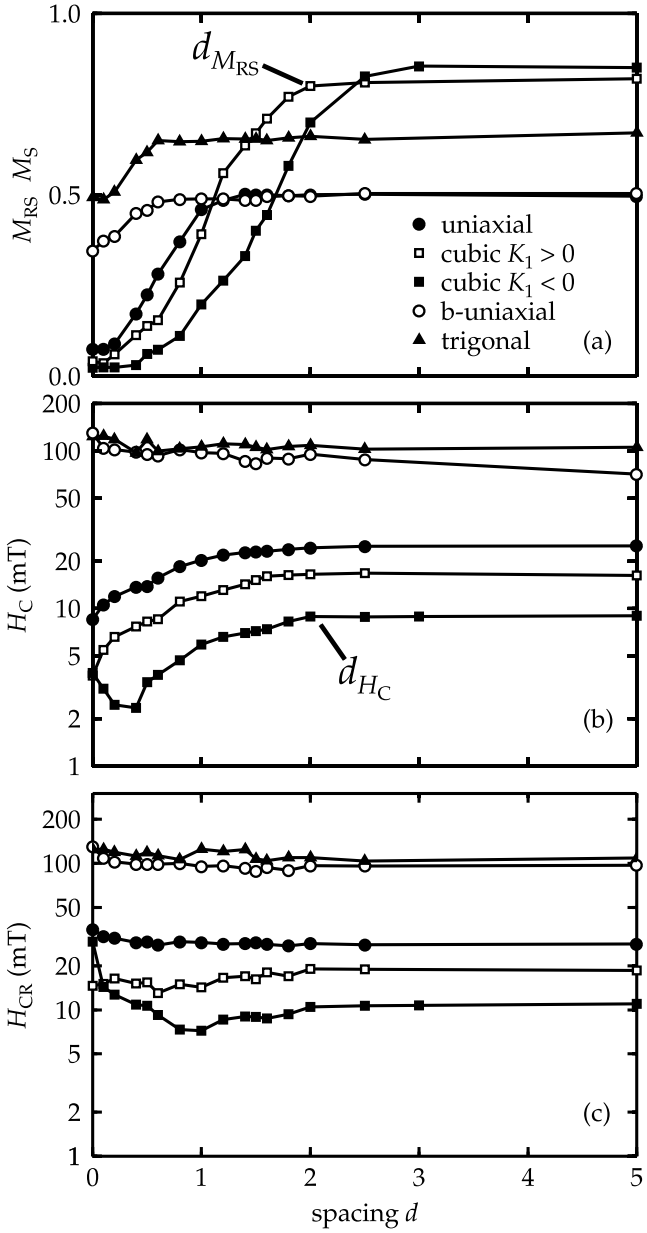

Figure 3. (a) M_{RS}/M_S, (b) H_C and (c) H_{CR} versus spacing d for five different anisotropy assemblages of ideal SD grains; uniaxial, cubic $K_1 > 1$, cubic $K_1 < 1$, b-uniaxial and trigonal. The anisotropy orientation of each assemblage is random.

and 0.866 respectively [*Kneller*, 1969; *Tauxe et al.*, 2002]. The trigonal anisotropy M_{RS}/M_S ratio agreed within two decimal places with theory, i.e., 0.65, and the b-uniaxial was 0.50 as expected from theory [*Dunlop*, 1971].

3.2. Anisotropy Control

[17] The effect of interactions is partially controlled by the type of anisotropy [*Kneller*, 1969]. If the anisotropy is restricted to the basal plane, then the effect of interactions is greatly reduced (Figure 3). This is point emphasized by considering $d_{M_{RS}}$, which for nonplanar anisotropies is greater than $d_{M_{RS}}$ for planar anisotropies (Table 1). As the order of anisotropy increases $d_{M_{RS}}$ decreases, e.g., $d_{M_{RS}}$ for uniaxial $< d_{M_{RS}}$ for cubic (8 fold). For all three nonplanar anisotropy regimes, $d_{H_C} > d_{M_{RS}}$ (Table 1), which suggests that H_C is more sensitive to interactions than M_{RS}/M_S. However, M_{RS}/M_S is clearly more strongly affected by the interactions. For example, for the cubic anisotropy with $K_1 > 0$, $M_{RS}/M_S \sim 0$ for $d < 0.3$, and equals 0.83 for the noninteracting regime, however, H_C increases from only ~4 mT to ~16 mT over the same range.

Table 1. Estimates for $d_{M_{RS}}$ and d_{H_C} for Ideal SD Grains[a]

Anisotropy	$d_{M_{RS}}$	d_{H_C}
Nonplanar Anisotropy		
uniaxial	1.2	2.0
cubic ($K_1 > 1$)	2.0	2.0
cubic ($K_1 < 1$)	2.5	2.0
Basal Plane Anisotropy		
b-uniaxial	0.6	...
trigonal	0.6	...

[a] $d_{M_{RS}}$ is the value of d in between $d = 0$ and 5, where M_{RS}/M_S becomes independent of interaction spacing (Figure 3a), similarly for H_C and d_{H_C} (Figure 3b).

3.3. Day Plots for Uniform SD Grains

[18] It is of interest to the paleomagnetist to plot simulated "Day plots", i.e., M_{RS}/M_S versus H_{CR}/H_C [*Day et al.*, 1977], with the effect of grain interaction spacing depicted (Figure 4). As the two planar and the two cubic anisotropies show similar behavior, only the b-uniaxial and cubic anisotropy with $K_1 < 0$ are plotted. The effect of decreasing d decreases M_{RS}/M_S and increases H_{CR}/H_C, causing the hysteresis parameters plot position to move from the

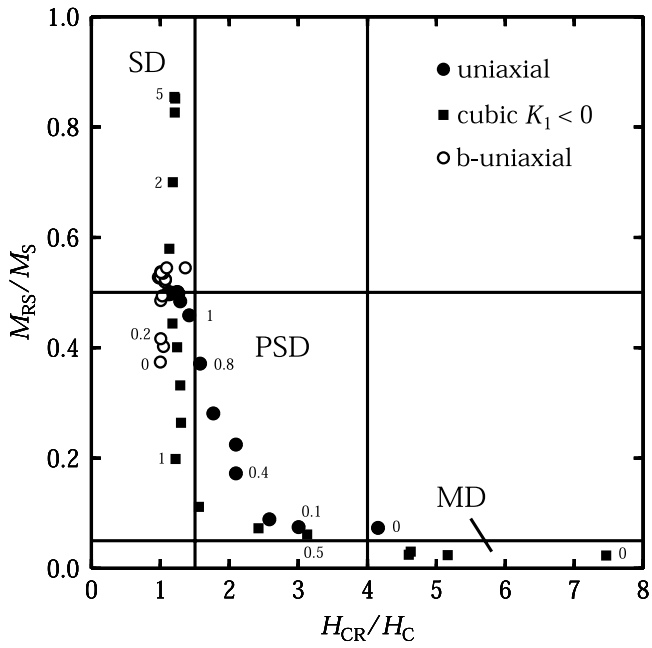

Figure 4. M_{RS}/M_S versus H_{CR}/H_C (Day plot) for three different anisotropy assemblages of ideal SD grains; uniaxial, cubic $K_1 < 1$ and b-uniaxial, with a range of interaction spacing; $0 \leq d \leq 5$. Some of the interaction spacings are marked. The effect of interactions is fairly consistent, so unmarked intermediate points have intermediate value of d. The anisotropy orientation of the assemblage is random.

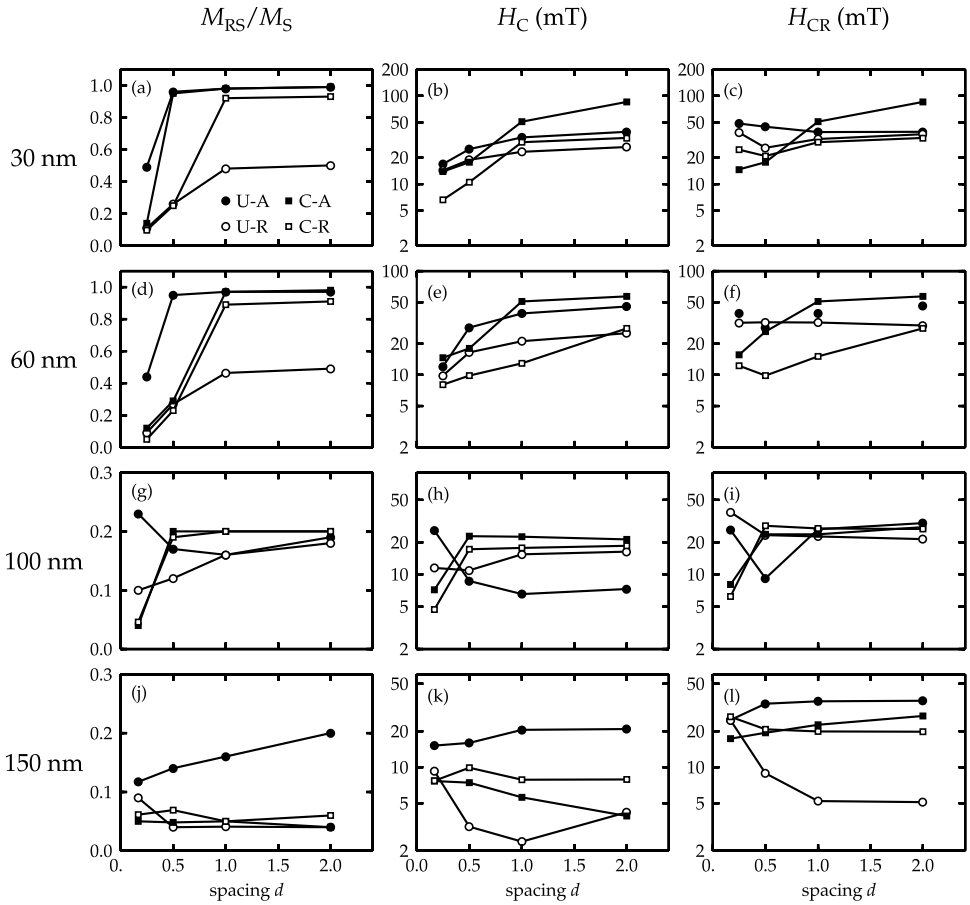

Figure 5. Calculated M_{RS}/M_S (first column), H_C (second column) and H_{CR} (third column) versus spacing d for assemblages with four different grain sizes; first row (a–c) 30 nm, second row (d–f) 60 nm, third row (g–i) 100 nm and the fourth row (j–l) 150 nm. Each assemblage consists of 64 cubic grains separated by distance d, with either uniaxial or cubic anisotropy and with both aligned or random anisotropy alignment. For the aligned anisotropy, the applied field was 5° from an easy axis.

traditional "SD region" toward the "MD region" as d is decreased. This behavior is more pronounced in the high-order nonplanar anisotropies than in the basal plane anisotropies. In particular cubic anisotropy with $K_1 < 0$, shifts from the traditional SD region through the PSD region and into the MD region. The b-uniaxial anisotropy position does not vary significantly with d. *Sprowl* [1990] found similar trends for his SD dipolar-interaction-field model.

4. Interactions Between Nonuniform SD Particles

[19] *Williams and Dunlop* [1989] demonstrated that in particles traditionally thought to be SD, the magnetization is not uniform, but there is "flowering" of the magnetic structure near the grain edges (Figure 1a.). The degree of flowering increasing with grain size until a vortex structure forms (Figure 1b). In this section the contribution of interactions to the hysteresis parameters of grains containing flower structures is examined.

[20] We consider assemblages of 64 cubic grains aligned in a regular cubic grid, i.e., $4 \times 4 \times 4$. In this system there are "two" kinds of interactions between the micromagnetic cells in the model; within the cubic grain there are both magnetostatic and exchange interactions, and between grains magnetostatic interactions.

[21] In the previous section the effect of grain size was normalized out of the model, however, for nonuniform structures the size of each grain is critical. We consider two cubic grain-sizes; 30 nm and 60 nm. In real magnetite grains, 30 nm is on the border of SP and stable-SD behavior [*Dunlop*, 1973], however, in the absence of thermal energy as in this model, there is no superparamagnetic/stable-SD threshold. In micromagnetic modeling the resolution of the model is very important and it has been shown that to accurately model a grain's structure it is necessary to have a resolution of two cells per exchange length [*Rave et al.*, 1998]. For a 30 nm grain the minimum resolution is $5 \times 5 \times 5$, while for a 60 nm grain it is $9 \times 9 \times 9$. To save CPU time and to model a range of different grain sizes and hysteresis, we used an individual grain size resolution of $4 \times 4 \times 4$. By implementing a slightly lower resolution, we have effectively underestimated the exchange energy. However, as we are primarily interested in changes with interaction spacing and for the Day plot simulations ratios, then our model will still show the same trends.

4.1. Assemblages of 30 nm Grains

[22] We have calculated the hysteresis parameters for interacting grains as a function of spacing (Figures 5a–5c). Four anisotropy regimes were modeled; uniaxial and

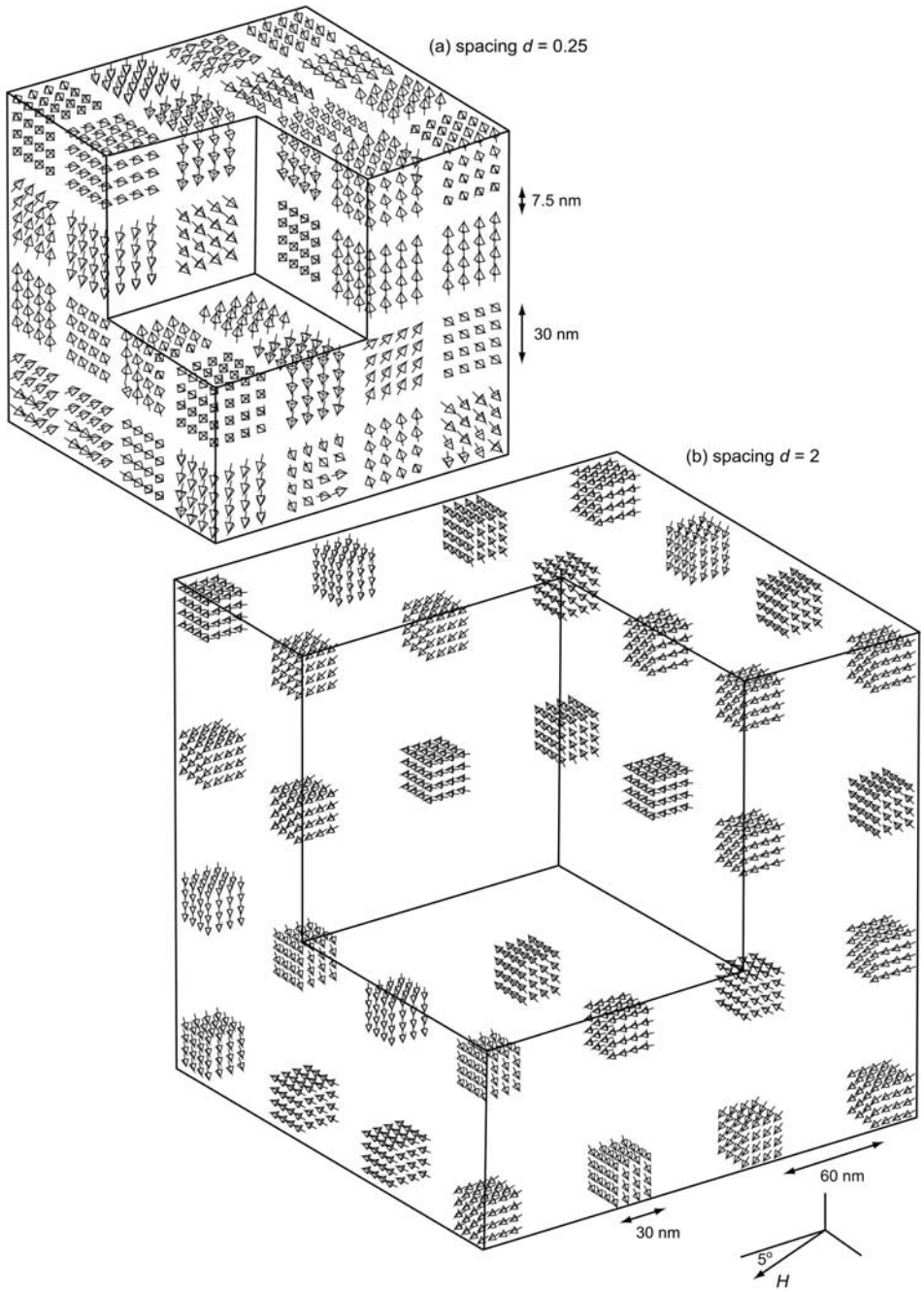

Figure 6. Two assemblages of 64, i.e., 4 × 4 × 4, 30 nm grains with randomly orientated uniaxial anisotropy: (a) interaction spacing $d = 0.25$ and (b) $d = 2$. Both structures are in the M_{RS}/M_S state, i.e., $H = 0$ during hysteresis. The field direction is marked.

cubic ($K_1 < 1$) anisotropies where each grain's anisotropy was either randomly aligned, or perfectly aligned with its neighbor and to within 5° of the applied field. Owing to the increased CPU time for the calculations of nonuniform structures, we have considered only four separate values of d.

[23] The effect of interactions is clearly seen if we compare the magnetic structure of a uniaxial random (U-R) state for a strongly interacting regime ($d = 0.25$) with a less interacting system $d = 2$, for $H = 0$ during hysteresis, i.e., the M_{RS} state (Figure 6). All the particles in both regimes are near-uniform SD grains with little flowering. For the $d = 2$ state, the particles are aligned with an easy uniaxial direction closest to the applied field direction, however, for $d = 0.25$ the magnetostatic energy dominates over the anisotropy energy and the overall magnetic structure is modified. The appearance of the $d = 0.25$ is more MD-like, however, there are no exchange interactions between grains. The grains near the edge of assemblage are aligned to minimize the total magnetic energy, reducing M_{RS}/M_S from 0.50 for $d = 2$ to 0.11 for $d = 0.25$.

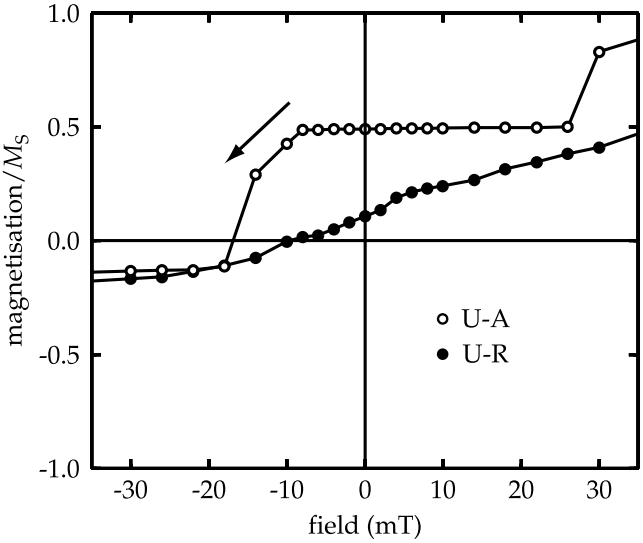

Figure 7. A simulated hysteresis curves for an assemblage of 64 30 nm uniaxial grains with interaction spacing d = 0.25 with aligned (a) and randomly (r) distributed anisotropy axis.

[24] The anisotropy alignment, i.e., U-R or uniaxial aligned (U-A), strongly affects the shape of the hysteresis loops for the interacting regime, i.e., $d = 0.25$ (Figure 7); the U-R hysteresis curve is smooth, and the aligned curve blocky. Such blocky hysteresis curves have been found previously in other micromagnetic studies of interacting aligned particles [*Ridley et al.*, 2002]. This effect is easily explained; in an assemblage of noninteracting identical aligned SW particles; each moment will flip coherently at the same field, i.e., the assemblage will behave like a single crystal. In the presence of interactions, each grain experiences an effective field which is a combination of the applied field and the magnetostatic interaction field. As the interaction field experienced by each grain can vary depending on position, each moment will rotate at different applied fields, giving rise to a blocky hysteresis curves. If the number of grains in the assemblage increases, then this effect will decrease.

[25] This effect was more pronounced in the uniaxial assemblage than the cubic one. The cubic regime has several intermediate states during rotation, i.e., the rotation is not instantaneous but occurs over a range of field steps. For $d = 0.5$ the effect of interactions is reduced and most of the grains rotate at the same field, giving a single step hysteresis curve.

[26] As d is increased both M_{RS}/M_S and H_C increase for all four anisotropy regimes (Figures 5a and 5b). This is associated with the more MD-like structure of the interacting assemblage (Figure 6). Randomizing the anisotropy directions decreases the absolute values of both M_{RS}/M_S and H_C, and increases interaction effects at larger d values. The behavior of H_{CR} is less consistent (Figure 5c): the cubic random (C-R) and cubic aligned (C-A) H_{CR} values increase with d. The U-A H_{CR} decreases gradually with d, while the U-R H_{CR} decreases initially, but then increases again slightly with d.

[27] M_{RS}/M_S for the U-R noninteracting (d = 2) grains is 0.50 in agreement with theory for ideal SD grains [*Wohlfarth and Tonge*, 1957; *Dunlop*, 1971]. However, for the C-R regime it was repeatably a little higher than the theoretical value (0.866) at 0.92. This difference is most likely to be due to the small assembly size, i.e., 64 particles.

4.2. Assemblages of 60 nm Grains

[28] The over-all hysteresis behavior of the 60 nm grains is similar to that of the 30 nm grains, however, M_{RS}/M_S is a little lower due to increased flowering of the domain structures regimes (Figures 5d–5f). The effect of anisotropy alignment, i.e., random or aligned, on the hysteresis curve for $d = 0.25$ for the 30 nm (Figure 7), was found to be similar for the 60 nm assemblages. However, for the 60 nm assemblage blocky hysteresis curves persisted to higher interaction spacings, i.e., $d = 0.5$.

[29] The M_{RS}/M_S ratio for the 60 nm assemblages appears to be more sensitive to interactions than the 30 nm case, e.g., for C-A with $d = 0.5$, $M_{RS}/M_S \sim 0.29$ for the 60 nm model, but ~0.95 for the 30 nm assemblage (Figures 5a and 5d).

4.3. Day Plots for Nonuniform SD Grains

[30] The general effect of interactions is to shift the hysteresis parameters' positions from the SD region toward the MD region on the Day plot for both the 30 nm and 60 nm assemblages (Figures 8a and 8b). The degree to which the hysteresis ratios move with interactions is dependent on the anisotropy type and its orientation, and grain size. As M_{RS}/M_S is significantly lower for the U-R regimes, these anisotropies plot lower on the Day plot than the U-A assemblages.

[31] For the 30 nm grains with U-A and C-R anisotropies, H_{CR}/H_C increases as d is decreased. The ratio H_{CR}/H_C for 30 nm aligned C-A does not vary significantly from unity and the effect of interactions is seen only in the variation of M_{RS}/M_S (Figure 8a). Generally, H_{CR}/H_C ratios for the 60 nm grains are slightly lower than for the 30 nm assemblage, especially for $d > 0.25$, and there is less dispersion along the H_{CR}/H_C axis (Figure 8b).

5. Interactions Between Pseudo-Single-Domain (PSD) Particles

[32] The effect of magnetostatic interactions on the hysteresis properties of assemblages of 100 nm and 150 nm cubic grains is considered in this section. In a noninteracting environment 100 nm grains can display both flower structures and vortex structures, however, at room temperature 150 nm grains only display vortex states (Figure 1). High-resolution models have shown that no other stable domain states exist in this grain size range for magnetite [*Muxworthy et al.*, 2003].

[33] The assemblages consisted of 64 grains placed on a 4 × 4 × 4 grid. Each cubic grain was represented by a resolution of 6 × 6 × 6. This is below the minimum resolution of two cells per exchange length; for a 100 nm grain the minimum resolution should be 15 × 15 × 15, and for 150 nm 23 × 23 × 23 [*Rave et al.*, 1998]. It was not practical to examine hysteresis parameters at these resolu-

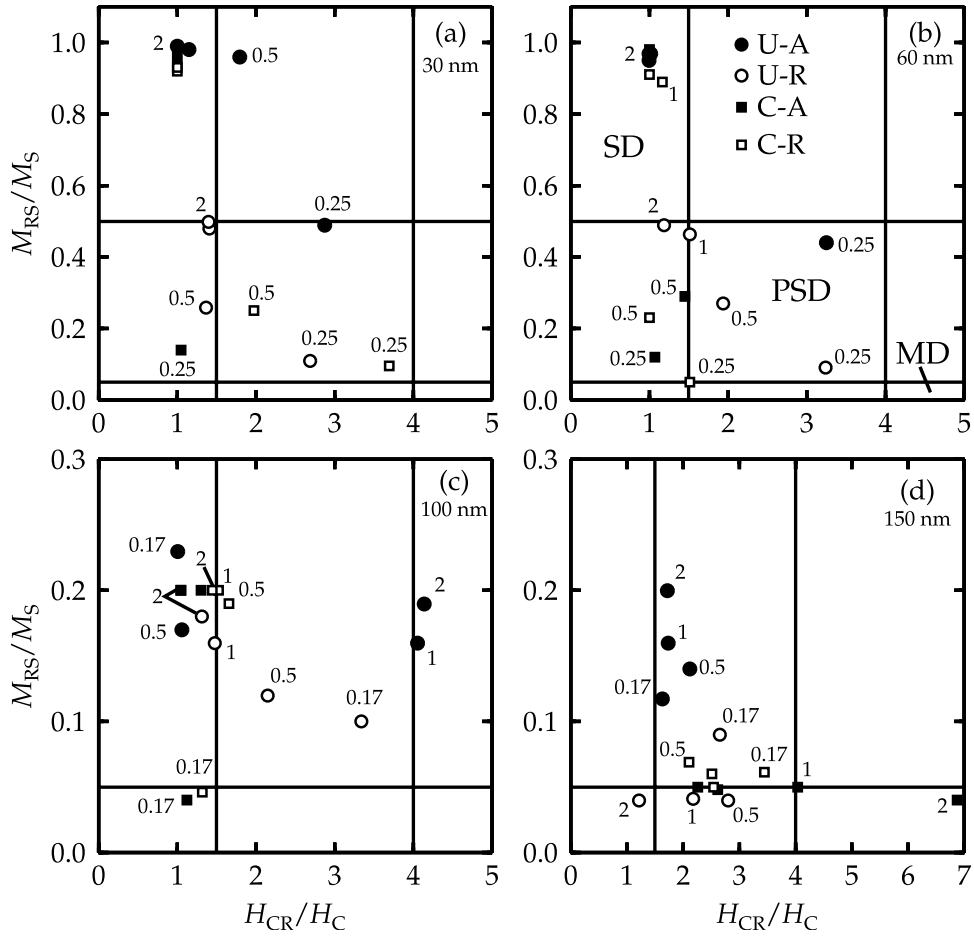

Figure 8. M_{RS}/M_S versus H_{CR}/H_C (Day plot) for assemblages of (a) 30 nm, (b) 60 nm (c) 100 nm and (d) 150 nm grains with various interaction spacings d. Each assemblage consists of 64 cubic grains separated by distance d, with four different anisotropies: U-A, U-R, C-A and C-R. For the aligned anisotropy, the applied field was 5° from an easy axis. Some of the interaction spacings are marked. The effect of interactions is fairly consistent, so unmarked intermediate points have intermediate value of d.

tions; for example, the largest interaction spacing considered for the 100 nm and 150 nm assemblages was $d = 2$. For a $6 \times 6 \times 6$ resolution, the total model resolution which includes the blank cells is $60 \times 60 \times 60$. If a resolution of $23 \times 23 \times 23$ had been used, then the model resolution would have been $230 \times 230 \times 230$.

[34] Another consideration is; how does significantly reducing the model resolution contribute to the interaction effects? For these grain size ranges only two types of magnetic structures can exist; SD/flower and vortex. In the SD/flower state, lowering the model resolution will cause the degree of flowering to be underestimated, increasing the calculated magnetic moment and consequently increasing the interaction field. In contrast for the vortex state, reducing the resolution will cause the magnetic moment calculated for the core to be lower, consequently the net magnetic moment of the grain will be underestimated, reducing a grain's interaction field. How these two features interact and affect the overall magnetic structure is uncertain; one decreasing and one increasing the interaction field. A true test of this is computationally unattainable at present. However, we believe our results will still display the correct trends, as the two possible states, i.e., flower and vortex, are still reasonably represented by this low resolution [*Muxworthy et al.*, 2003].

5.1. Assemblages of 100 nm Grains

[35] The effect of interactions is clearly seen by examining the M_{RS} domain states for a U-A regime with $d = 1/6$ and 0.5 (Figure 9). For $d = 1/6$, each grain displays a flower or SD state. For $d = 0.5$, some grains are in the vortex state. Decreasing d effectively increases the SD threshold size, r_0, i.e., the SD to MD transition size, which for noninteracting cubic magnetite is ~70 nm [*Williams and Wright*, 1998]. The external field a grain experiences, whether it be an applied external field or a local interaction field, has the effect of shifting a grain's domain structure to a more saturated one [*Williams and Dunlop*, 1995]. For grains very close to r_0, the local interaction field is sufficient to saturate the domain structure. This change in r_0, is clearly observed in the 100 nm particles which switch by noncoherent rotation in the noninteracting state, but by coherent rotation in the interacting regimes giving rise to blocky hysteresis loops similar to Figure 7.

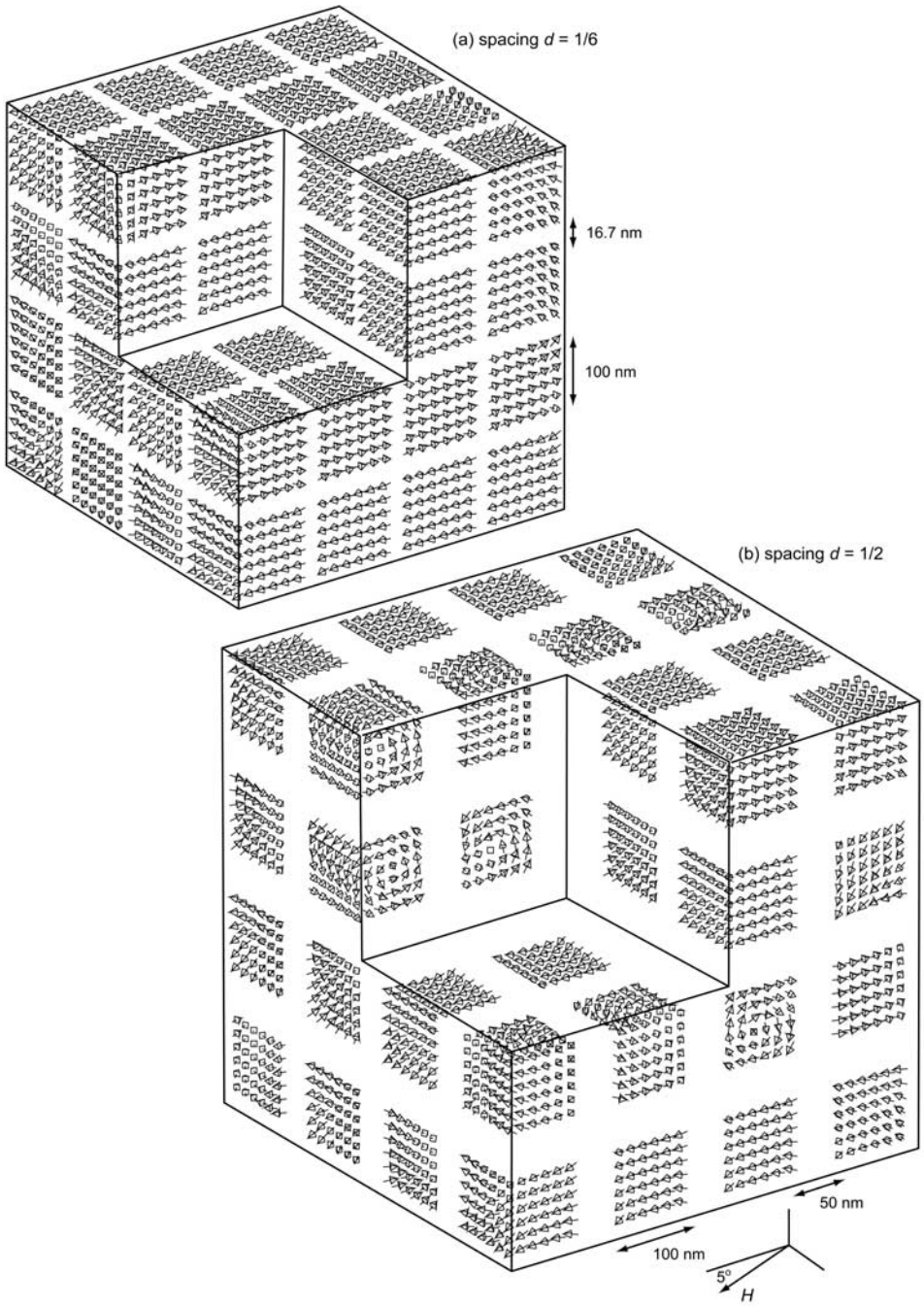

Figure 9. Two assemblages of 64, i.e., 4 × 4 × 4, 100 nm grains with U-A: (a) interaction spacing d = 1/6 and (b) d = 1/2. Both structures are in the M_{RS}/M_S state, i.e., H = 0 during hysteresis. The anisotropy is aligned to within 5° of the applied field. The field direction is marked.

[36] The effect of interactions is to increase M_{RS}/M_S and H_C for the U-A regime, but to decrease it for the U-R one (Figures 5g and 5h). For a U-A assemblage with the anisotropy aligned to within 5° of the applied field, the interaction field experienced by an individual grain is on average aligned close to the applied field. Whereas, for the U-R assemblage the anisotropy has no preferred direction. In both regimes, when the external field is decreased then the relative importance of the anisotropy and interaction field increases. If the interaction field is aligned with the effective anisotropy field, the height of the observed energy barrier restricting rotation is increased. It is more likely in the random anisotropy regime, for the anisotropy field and the interaction field to be pointing in different directions, making the observed potential energy well in the random state shallower.

[37] For large d (noninteracting), U-R H_C is greater than U-A H_C (Figure 5h), even though M_{RS}/M_S is larger for the U-A assemblage. This is probably related to the importance of field angle and nucleation of the vortex state [*Hubert and*

Rave, 1999]. For the U-A H_{CR} decreases initially as d is increased (Figure 5i). It then increases and remains constant with little variation with d.

[38] The hysteresis parameters for the cubic anisotropy regimes display a more consistent behavior with increasing d (Figures 5g–5i). M_{RS}/M_S, H_C and H_{CR} all initially increase with increasing d, but appear to be almost independent of interactions for $d > 0.5$.

5.2. Assemblages of 150 nm Grains

[39] As d increases, M_{RS}/M_S, H_C and H_{CR} increase for the U-A assemblage. (Figures 5j–5l). H_C and H_{CR} for the U-R assemblage both increase sharply as d is decreased. For the cubic regimes, M_{RS}/M_S is almost independent of d, H_C increases with d and H_{CR} decreases for C-R, but increases for C-A.

[40] For highly interacting states, flower states were observed in some of the grains in the assemblage, however, unlike the 100 nm assemblage, these grains rotate noncoherently. No blocky hysteresis curves were observed (*cf*. Figure 7).

5.3. Day Plots for PSD Grains

[41] For both the 100 nm and 150 nm assemblages plot much lower on the Day plot, as $M_{RS}/M_S \ll 0.5$ for $d = 2$ because of the existence of vortex states (Figures 8c and 8d).

[42] The 100 nm U-R assemblage displays similar behavior to the 30 nm and 60 nm Day plots (Figures 8a and 8b). As d is decreased M_{RS}/M_S decreases and H_{CR}/H_C increases, and the hysteresis parameters move toward the MD region. The 100 nm U-A displays completely opposite behavior: H_{CR}/H_C decreases with increases d, while M_{RS}/M_S does not vary significantly (Figure 8c). This decrease in H_{CR}/H_C is due to the increase in H_C with increasing interactions, and reflects the apparent increase in r_0. The cubic anisotropies both display similar behavior: M_{RS}/M_S increases as d is increased and there is little variation in H_{CR}/H_C with interaction.

[43] Generally, for the 150 nm assemblages (apart from the C-A model), for decreasing d little change is found: M_{RS}/M_S and H_{CR}/H_C decrease slightly or do not vary (Figure 8d). For the 150 nm C-A assemblage, as d increases H_{CR}/H_C increases, that is, as magnetostatic interactions increase the grains becomes more SD-like in similar manner to the 100 nm U-A assemblage (Figure 8c), and grains which display noncoherent rotation behavior for large d, rotate coherently when there is a large magnetostatic field.

6. Discussion

[44] There are some general trends which are found in the models; interactions between SD grains (either uniform (section 3) or nonuniform (section 4)) decrease both M_{RS}/M_S and H_C (Figures 3 and 5), regardless of the type or orientation of the anisotropy. The decrease in M_{RS}/M_S is also generally observed for small PSD grains (Figures 5g and 5j), though, there are exceptions to this, e.g., the 100 nm U-A assemblage (Figure 5g). For the PSD grains H_C displays less consistent dependency on interactions (Figures 5h and 5k).

[45] The behavior of H_{CR} is more complicated. For uniform and nonuniform SD grains with random anisotropy, H_{CR} increases as the interaction spacing becomes small (Figures 3 and 5). Above $d \sim 0.5$, H_{CR} can increase or decrease depending on the anisotropy. In the 100 nm grain assemblages interactions increase H_{CR} in the uniaxial models, but decrease H_{CR} in the cubic assemblages. In the 150 nm assemblages, interactions increase H_{CR} in the random anisotropy systems, but decrease it in the aligned anisotropy assemblages (Figures 5i and 5l).

[46] The uniform and nonuniform (flower) randomly orientated SD grains display similar hysteresis behavior, however, the absolute hysteresis values are a little higher for the flower structures. This maybe due to the low number of grains in the nonuniform model, alternatively it may be a real effect like configurational anisotropy.

[47] The configurational anisotropy is a term coined to describe the energy barrier associated with intermediate states in a transition path. Temporarily ignoring magnetocrystalline anisotropy, consider a SD-like or flower-state in a cubic grain (Figure 1a). The energy of a SD state aligned along x or y are equivalent due to symmetry; the degree of flowering will be identical. For a SD to rotate coherently from the x direction to the y direction or vice versa it will have to pass through an intermediate state. The degree of flowering varies depending on the direction of the magnetization with respect to the cube faces. Intermediate states have less flowering due to geometry considerations giving rise to an effective energy barrier. If no flowering occurs, i.e., a uniform SD grain, then for cubic grains with no magnetocrystalline anisotropy there would be no energy barrier for this rotation. However, in magnetite, flowering is in reality common. Since the degree of flowering increases as the grain size increases, the energy barrier along the transition path increases. This effect occurs for other types of transitions, e.g., between vortex states. Configurational anisotropy will always exist in cubic structures, but will often be masked by magnetocrystalline anisotropy or another anisotropy created by applied fields. Only a sphere will have no configurational anisotropy.

6.1. Effect of Anisotropy and Disorder

[48] The reversal mechanism and hysteresis parameters are sensitive to both the type and disorder of the intrinsic material properties. In the case of anisotropy-type, increasing the degrees of freedom increases the effect of interactions.

[49] Aligning the anisotropy increases the interaction field, which has the effect of stabilizing states during the reversal process and leads to highly symmetric co-operative reversals of each grain's moment. A random anisotropy breaks this symmetry significantly to reduce switching, leading to a relatively random reversal of individual elements.

[50] The importance of anisotropy size and order, and interactions is most strongly seen in the PSD grains, i.e., grains which can display a vortex state when not in the presence of interactions; the effect of interactions can make assemblages either more SD-like or MD-like (Figure 8). PSD grains become more SD-like when the anisotropy of each grain is aligned; r_0 is effectively increased.

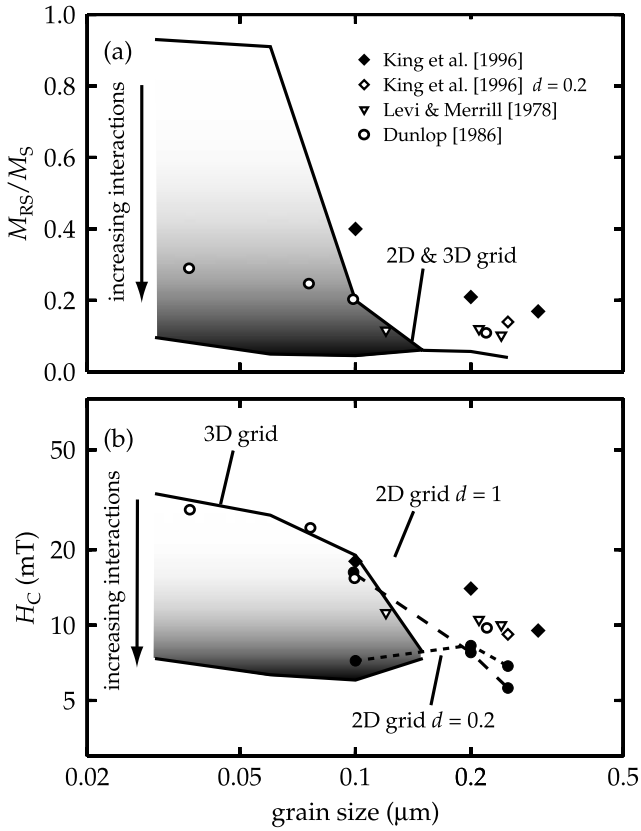

Figure 10. Hysteresis parameters (a) M_{RS}/M_S and (b) H_C versus grain size for micromagnetic simulations and experimental data. In (a) the 2D and 3D micromagnetic results are plotted on top of each other, and a single envelope is shown (on the lower curve for grains <100 nm, d = 0.25, for grains >100 nm d = 1/6). In (b) only the 3D data is shown as an envelope. In both (a) and (b), on the lower curve for grains <100 nm d = 0.25, for grains $\geq$100 nm d = 1/6 or 1/5. The samples of *King et al.* [1996] were produced by EBL; three samples were "noninteracting" while the 250 nm sample had a spacing of 0.2. The samples of *Levi and Merrill* [1978] and *Dunlop* [1986] were grown magnetites.

[51] The increase in r_0 as the interaction spacing is decreased for aligned anisotropy, may explain why some magnetotatic bacteria possess aligned grains of magnetite above the traditional value for $r_0 \sim 70$ nm [*McCartney et al.*, 2001]. By aligning the anisotropies, the grains become stable SD, and having larger crystals will increase the magnetic signal.

6.2. Comparison With Experimental Data

[52] Several experimental tests for interactions have been developed, e.g., Henkel plots [*Henkel*, 1964], however, all these methods produce nonunique solution. One of the reasons for this is the actual testing of a given method; it is experimentally difficult to control the interaction spacing, though it is possible with lithographic techniques.

[53] King and co-workers [*King et al.*, 1996; *King and Williams*, 2000] produced two-dimensional (2D) grids of identical cubic magnetite crystal samples by electron beam lithography (EBL) with a range of controlled interaction spacings. We have simulated the hysteresis parameters of these samples, using 4 × 4 grids of 100 nm, 200 nm and 250 nm cubic grains with a grain resolution of 10 × 10 × 10, for two values of d per grain size (d = 0.2 and 1). We assumed a random uniaxial anisotropy regime. H_C and M_{RS}/M_S were determined for hysteresis parallel to the plane of the sample following *King et al.* [1996].

[54] M_{RS}/M_S and H_C are plotted versus grain size for the modeled 2D and 3D arrays and a range of experimental samples including the EBL samples of *King et al.* [1996], and dispersed grown samples of *Dunlop* [1986] and *Levi and Merrill* [1978] (Figure 10).

[55] For simulations for grains <100 nm, M_{RS}/M_S and H_C both display a strong dependency on d. Almost the entire range of M_{RS}/M_S is covered by variations in d (Figure 10). From the M_{RS}/M_S data it appears that the *Dunlop* [1986] samples have a moderate interaction spacing, which on comparison with Figure 5, it is suggested that d is between 0.25–0.5, however, from the H_C data they appear to be nearly noninteracting (Figure 10b).

[56] For the experimental samples between 100–150 nm, M_{RS}/M_S and H_C agree well with the noninteracting models. The measured H_C for King's 100 nm sample, and the simulated H_C for a 100 nm 2D grid, are remarkably close (Figure 10b).

[57] For the assemblages >150nm, M_{RS}/M_S for the interacting and noninteracting regimes converge, and plot below the experimental data. M_{RS}/M_S for the data of *King et al.* [1996] is greater than that of the other experimental data and the model results. This difference is attributed to high levels of stress within the samples; King found that his EBL samples displayed magnetic behavior consistent with high-stress material. He suggested that these stresses originated in the production processes, where thin-films of iron are oxidized to magnetite.

[58] In agreement with the 3D calculations the effect of interactions in the 250 nm regime is to increase H_C (Figure 10). The H_C data for the model 2D grids plots a little below the experimental data. For example, on comparison with King's noninteracting samples, the model for the 0.1 μm regime with d = 1, predicts $H_C \sim 16$ mT compared to a measured value of 18 mT, and for the 0.2 μm grid the model gave $H_C \sim 8$ mT versus a measured value of 14 mT. These differences may be due to several factors; for the samples of *King et al.* [1996] the discrepancy is likely to be due to stress. For the samples of *Dunlop* [1986] and *Levi and Merrill* [1978] the difference maybe due to comparing assemblages of identical crystals in the model with samples which have distributions of both grain size and coercive force. It is likely that the samples with mean sizes >100 nm have some stable SD grains within them, and *vice versa*, which will strongly effect M_{RS}/M_S and H_C.

6.3. Reinterpreting the Day Plot

[59] *Dunlop* [2002] simulated Day plots using an analytical mixing model for noninteracting SD and MD grains. He showed that nonlinear combinations of classical SD and MD theory can adequately explain the observed behavior in the PSD region, i.e., Dunlop suggests that PSD behavior is due to SD-like areas within a MD structure. These SD-like

areas could be associated with inclusions or imperfections within the crystal or due domain walls themselves displaying SD-like characteristics. Alternatively, Dunlop's approach can be seen simply as a bimodal distribution model.

[60] In contrast, 3D micromagnetic modeling suggests that PSD behavior is a real phenomenon and can be described by individual or noninteracting small MD grains that display curling mechanisms of reversal [this paper, *Newell and Merrill*, 2000].

[61] Interactions between SD grains can also generate such PSD-behavior, as was first shown by *Sprowl* [1990] and is supported by the more rigorous calculations made in this paper (Figures 4 and 8). That touching or at least strongly interacting SD particles display MD-like characteristics is from a theoretical point of view not surprising, as the main difference between an assemblage of interacting grains and a single MD grain is simply the presence or absence of the exchange energy. The assemblage of interacting SD grains and the MD particle will not have the same internal structure, but their behavior will be similar as the total magnetostatic energies are identical.

[62] Initially, from the results in this study, the Day plot does not seem to provide a unique solution; however, if the grain size distribution and the dominant anisotropy of a sample can be determined by some independent method then the effect of interactions can be assessed from the Day plot.

7. Conclusions

[63] The effect of magnetostatic interactions in assemblages of magnetite-like minerals has been systematically studied: we have considered variations in grain size, spacing and anisotropy size and order. Several key features have been observed; the effect of interactions for small SD grains (either uniform or nonuniform) is to decrease M_{RS}/M_S and H_C and to increase the ratio H_{CR}/H_C. On the Day plot the samples shift from the traditional SD regions to the PSD and MD regions as inter-grain spacing decreases (Figures 4 and 8).

[64] The effect of interactions on the PSD grains, i.e., grains which can display a vortex state when not in the presence of interactions, depends strongly on orientation of the anisotropy, its type and the grain size; the effect of interactions can make assemblages either more SD-like or MD-like (Figure 8). It is shown that for assemblages of aligned magnetite particles, that as the interaction spacing is decreased, the SD/MD transition size increases, i.e., $r_0 >$ 70 nm. This may explain why some magnetotatic bacteria possess aligned grains of magnetite above 70 nm; by aligning the anisotropies, the grains become stable SD, and having larger crystals will increase the magnetic signal.

[65] **Acknowledgments.** This paper benefited from comments from David Dunlop, Mike Jackson, and Phil Wannamaker. This work was funded by research grant NER/A/S/2001/00539 to W.W.

References

Bertram, H. N., and A. K. Bhatia, The effect of interactions on the saturation remanence of particulate assemblies, *IEEE Trans. Magn.*, *9*, 127–133, 1973.

Brown, W. F., Jr., *Micromagnetics*, John Wiley, Hoboken, N. J., 1963.

Davis, P. M., Effects of interaction fields on the hysteresis properties of assemblies of randomly orientated magnetite or electric moments, *J. Appl. Phys.*, *51*(1), 594–600, 1980.

Day, R., M. Fuller, and V. A. Schmidt, Hysteresis properties of titanomagnetites: Grain-size and compositional dependence, *Phys. Earth Planet. Inter.*, *13*, 260–266, 1977.

Dormann, J. L., L. Bessais, and D. Fiorani, A dynamic study of small interacting particles-superparamagnetic model and spin-glass laws, *J. Phys. C Solid State Phys.*, *21*, 2015–2034, 1988.

Dunlop, D. J., Magnetic properties of fine-particle hematite, *Ann. Géophys.*, *27*, 269–293, 1971.

Dunlop, D. J., Superparamagnetic and single-domain threshold sizes in magnetite, *J. Geophys. Res.*, *78*, 1780–1793, 1973.

Dunlop, D. J., Hysteresis properties of magnetite and their dependence on particle-size - a test of pseudo-single-domain remanence models, *J. Geophys. Res.*, *91*(B9), 9569–9584, 1986.

Dunlop, D. J., Theory and application of the Day plot (M_{rs}/M_s versus H_{cr}/H_c): 1. Theoretical curves and tests using titanomagnetite data, *J. Geophys. Res.*, *107*(B3), 2056, doi:10.1029/2001JB00486, 2002.

Dunlop, D. J., and G. West, An experimental evaluation of single-domain theories, *Rev. Geophys.*, *7*, 709–757, 1969.

Fabian, K., and F. Heider, How to include magnetostriction in micromagnetic models of titanomagnetite grains, *Geophys. Res. Lett.*, *23*(20), 2839–2842, 1996.

Fletcher, E. J., and W. O'Reilly, Contribution of Fe^{2+} ions to the magnetocrystalline anisotropy constant K_1 of $Fe_{3-x}Ti_xO_4 (0 < x < 0.1)$, *J. Phys. C Solid State Phys.*, *7*, 171–178, 1974.

Heider, F., and W. Williams, Note on temperature dependence of exchange constant in magnetite, *Geophys. Res. Lett.*, *15*(2), 184–187, 1988.

Henkel, O., Remanenzverhalten und Wechselwirkung in hartmagnetischen Teilchenkollektiven, *Phys. Status Solidi*, *7*, 919–924, 1964.

Hubert, A., and W. Rave, Systematic analysis of micromagnetic switching processes, *Phys. Status Solidi B*, *211*, 815–829, 1999.

Hwang, M., M. C. Abraham, T. A. Savas, H. I. Smith, R. J. Ram, and C. A. Ross, Magnetic force microscopy study of interactions in 100 nm period nanomagnet arrays, *J. App. Phys.*, *87*(9), 5108–5110, 2000.

King, J. G., and W. Williams, Low-temperature magnetic properties of magnetite, *J. Geophys. Res.*, *105*(B7), 16,427–16,436, 2000.

King, J. G., W. Williams, C. D. W. Wilkinson, S. McVitie, and J. N. Chapman, Magnetic properties of magnetite arrays produced by the method of electron beam lithography, *Geophys. Res. Lett.*, *23*(20), 2847–2850, 1996.

Kneller, E., Fine particle theory, in *Magnetism and Metallurgy*, edited by A. Berkowitz and E. Kneller, pp. 366–472, Academic, San Diego, Calif., 1969.

Levi, S., and R. T. Merrill, Properties of single domain, pseudo-single domain, and multidomain magnetite, *J. Geophys. Res.*, *83*, 309–323, 1978.

McCartney, M. R., U. Lins, M. Farina, P. R. Buseck, and R. B. Frankel, Magnetic microstructure of bacterial magnetite by electron holography, *Eur. J. Mineral.*, *13*(4), 685–689, 2001.

Muxworthy, A. R., Effect of grain interactions on the frequency dependence of magnetic susceptibility, *Geophys. J. Int.*, *144*(2), 441–447, 2001.

Muxworthy, A. R., and W. Williams, Micromagnetic calculation of coercive force as a function of temperature in pseudo-single domain magnetite, *Geophys. Res. Lett.*, *26*(8), 1065–1068, 1999.

Muxworthy, A. R., D. J. Dunlop, and W. Williams, High-temperature magnetic stability of small magnetite particles, *J. Geophys. Res.*, *108*(B5), 2281, doi:10.1029/2002JB002195, 2003.

Néel, L., Théorie du traînage magnétique des ferromagnétiques en grains fins avec applications aux terres cuites, *Ann. Géophys.*, *5*, 99–136, 1949.

Newell, A. J., and R. T. Merrill, Size dependence of hysteresis properties of small pseudo-single-domain grains, *J. Geophys. Res.*, *105*(B8), 19,393–19,403, 2000.

Pauthenet, R., and L. Bochirol, Aimantation spontanée des ferrites, *J. Phys. Rad.*, *12*, 249–251, 1951.

Rave, W., K. Fabian, and A. Hubert, The magnetic states of small cubic magnetic particles with uniaxial anisotropy, *J. Magn. Magn. Mater.*, *190*, 332–348, 1998.

Ridley, P. H. W., G. W. Roberts, and R. W. Chantrell, Simulation of the micromagnetic behavior of arrays of interacting nanoelements, *J. App. Phys.*, *92*(2), 1069–1077, 2002.

Ross, C. A., et al., Magnetic behavior of lithographically patterned particle arrays (invited), *J. App. Phys.*, *91*(10), 6848–6853, 2002.

Shcherbakov, V. P., B. E. Lamash, and N. K. Sycheva, Monte-Carlo modeling of thermoremanence acquisition in interacting single-domain grains, *Phys. Earth Planet. Inter.*, *87*, 197–211, 1995.

Shcherbakov, V. P., N. K. Sycheva, and B. E. Lamesh, Monte Carlo modeling of TRM and CRM acquisition and comparison of their properties in

an ensemble of interacting SD grains, *Geophys. Res. Lett.*, *23*(20), 2827–2830, 1996.

Shcherbakov, V. P., B. E. Lamash, and N. K. Sycheva, The magnetic susceptibility and viscous magnetization of interacting single-domain grains, *Izv. Phys. Solid Earth*, *36*(5), 430–436, 2000.

Spinu, L., and A. Stancu, Modeling magnetic relaxation phenomena in fine particles systems with a Preisach-Néel model, *J. Magn. Magn. Mater.*, *189*, 106–114, 1998.

Sprowl, D. R., Numerical estimation of interactive effects in single-domain magnetite, *Geophys. Res. Lett.*, *17*(11), 2009–2012, 1990.

Stoner, E. C., and E. P. Wohlfarth, A mechanism of magnetic hysteresis in heterogeneous alloys, *Philos. Trans. R. Soc. London, Ser. A*, *240*, 599–602, 1948.

Tauxe, L., H. N. Bertram, and C. Seberino, Physical interpretation of hysteresis loops: Micromagnetic modeling of fine particle magnetite, *Geochem. Geophys. Geosyst.*, *10*(3), 1055, doi:10.1029/2001GC000241, 2002.

Virdee, D., The influence of magnetostatic interactions on the magnetic properties of magnetite, Ph.D. thesis, Univ. of Edinburgh, Edinburgh, UK, 1999.

Williams, W., and D. J. Dunlop, Three-dimensional micromagnetic modeling of ferromagnetic domain structure, *Nature*, *337*, 634–637, 1989.

Williams, W., and D. J. Dunlop, Simulation of magnetic hysteresis in pseudo-single-domain grains of magnetite, *J. Geophys. Res.*, *100*(B3), 3859–3871, 1995.

Williams, W., and T. M. Wright, High-resolution micromagnetic models of fine grains of magnetite, *J. Geophys. Res.*, *103*(B12), 30,537–30,550, 1998.

Winklhofer, M., K. Fabian, and F. Heider, Magnetic blocking temperatures of magnetite calculated with a three-dimensional micromagnetic model, *J. Geophys. Res.*, *102*(B10), 22,695–22,709, 1997.

Wohlfarth, E. P., and D. G. Tonge, The remanent magnetization of single-domain ferromagnetic particles, *Philos. Mag.*, *2*, 1333–1344, 1957.

Wright, T. M., W. Williams, and D. J. Dunlop, An improved algorithm for micromagnetics, *J. Geophys. Res.*, *102*(B6), 12,085–12,094, 1997.

A. Muxworthy, D. Virdee, and W. Williams, Institute of Earth Sciences, University of Edinburgh, King's Buildings, West Mains Road, Edinburgh, EH9 3JW, UK. (adrian.muxworthy@ed.ac.uk)